SC Advances (Electronic Supplementary Information)

Photochemical *anti-syn* isomerization around the –N–N= bond in heterocyclic imines

Michal Hricovíni, [a] James Asher [b] and Miloš Hricovíni *[c]

Institute of Chemistry, Slovak Academy of Sciences, Dúbravská cesta 9, 845 38 Bratislava, Slovak Republic.
Institute of Inorganic Chemistry, Slovak Academy of Sciences, Dúbravská cesta 9, 845 36 Bratislava, Slovak Republic.
Institute of Chemistry, Slovak Academy of Sciences, Dúbravská cesta 9, 845 38 Bratislava, Slovak Republic. E-mail: milos.hricovini@savba.sk; Fax: +421-2-594 0222; Tel: +421-2-59510323.

SUPPLEMENTARY INFORMATION S1: ADDITIONAL COMPUTATIONAL RESULTS

The computational methods used will be abbreviated as in the main paper:

- ωB97XD/LANL2DZ = WB-L2
- ωB97XD/6-311++G(2d,2p) = WB-6+
- CCSD//cc-pVDZ = CC-DZ
- CCSD//cc-pVTZ = CC-TZ

These will be combined either with PCM or SMD to simulate the DMSO solvent environment. Additionally, CASSCF will also be used, primarily to examine excited states. The details are as follows.
CASSCF calculations were performed in OpenMolcas with PCM (SMD was not available). The cc-pVTZ basis was used. Natural orbitals from a UHF calculation, with the IVO keyword for improved virtual orbitals, were used as a starting point. The calculation then gradually expanded the active space, in the sequence CAS[4,4], CAS[6,8], CAS[8,12]. State-averaging was performed over the first three states (GS, ES1, ES2). The structure of the molecule was not reoptimised; the structures were taken from the WB-6+ optimizations.
Generally, the excited-state calculations were highly sensitive to the choice of active space.

1. BENCHMARKING

1.1 Model 1 (**M1**)

Table S1. Properties of the potential energy curve of **M1**, calculated at different levels of theory. Energies are in kJ/mol. "Barrier" refers to the energy maximum. CAS[8,12] calculations use geometries optimised with WB-6+; in all other cases, energies given are from optimization of both electronic and molecular structure with the specified method.

Property:	WB-L2		WB-6+		CC-DZ		CC-TZ	
	PCM	SMD	PCM	SMD	PCM	SMD	PCM	SMD
E_{syn}-E_{anti}	1.6	3.9	7.9	10.5	7.1	9.3	7.4	9.8
$E_{barrier}$-E_{syn}	26.0	24.3	18.0	15.6	18.6	15.5	18.4	16.2
$E_{barrier}$-E_{anti}	27.6	28.2	25.9	26.1	25.7	24.7	25.8	26.0
barrier angle	103˚	104˚	109˚	107˚	109˚	106˚	106˚	104˚

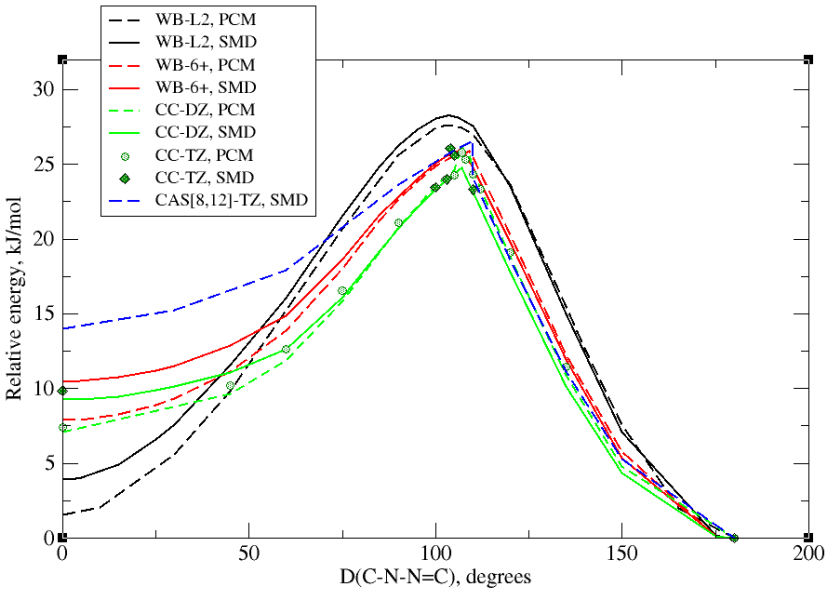

Figure S1. Potential energy curves of **M1**, calculated at different levels of theory (with geometry also optimized at the specified level of theory, except for CAS[8,12]-TZ, PCM, which used molecular geometries from WB-6+/SMD). The energy is plotted relative to that of the *anti*-form (180˚).

We note here that the ground-state energy curve consists of two intersecting curves distinguished by the *D*(H-N-N=C) dihedral angle. At *syn*, this angle is 180˚, but it decreases to about 104˚ with increasing D(C-N-N=C). At *anti*, this angle is 0 ˚, but it increases to about 70˚ with decreasing D(C-N-N=C). The two energy curves cross at D(C-N-N=C) = 107˚. However, there is a small energy barrier of 0.9 kJ/mol between these two curves at 107˚; for this reason, simply plotting the lowest energy possible for a given D(C-N-N=C) dihedral angle (as in Fig. S1) does not capture the whole of the energy barrier. (Or, put differently, the dihedral angle is not *exactly* the same as the reaction coordinate for *anti-syn* isomerization, merely a close approximation to it.) Fig. S2 shows the two structures at 107˚, as well as the energy curve (WB-6+ level).
It should also be noted that, although these two curves meet at 107˚ for the ground-state energy, they are not guaranteed to meet here (or anywhere else) for any other properties calculated from the geometries for these two curves. Thus, kinks and discontinuities may occur in vertical excitation energy curves, as well as in cases where the electronic structure and molecular geometry are optimised using different methods or levels of theory.

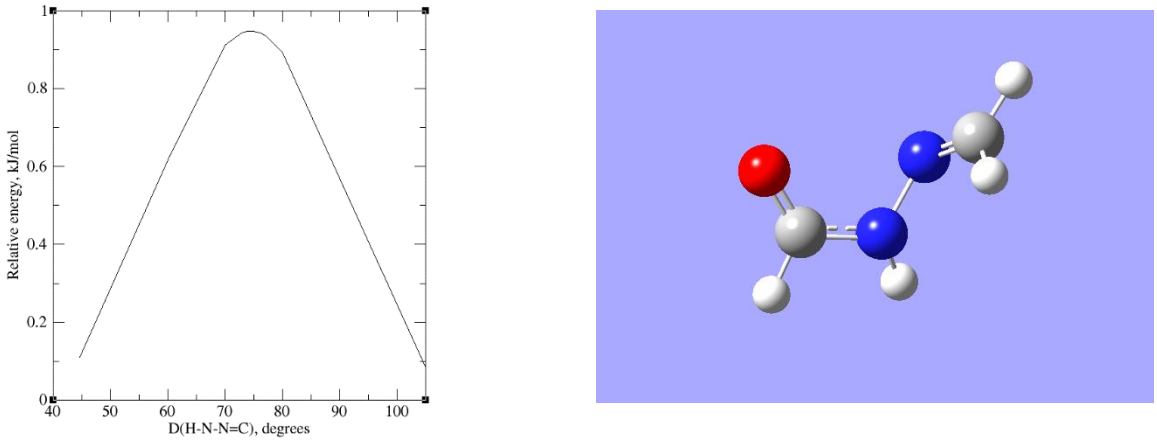

Figure S2. Details of the transition state. Left: potential energy curve of **M1** for transition between the two parts of the WB-6+ curves at 107˚. Right: **M1** at 107˚, coming from anti-conformation.

1.2 Model 2 (**M2**)

Table S2. Properties of the potential energy curve of **M2**, calculated at different levels of theory. Energies are in mH; angles are in degrees. "Barrier" refers to the smaller energy maximum.

Property:	WB-L2		WB-6+		CC-DZ
	PCM	SMD	PCM	SMD	SMD
E_{syn}-E_{anti}	-1.4	-0.5	6.1	6.6	1.2
$E_{barrier}$-E_{syn}	20.7	18.6	11.1	9.0	10.3
$E_{barrier}$-E_{anti}	19.3	18.0	17.2	15.5	11.5
syn- angle	6˚	6˚	15˚	51˚	57˚
anti- angle	-170˚	-172˚	-171˚	-170˚	-169˚
barrier angle	117˚	120˚	120˚	121˚	153˚

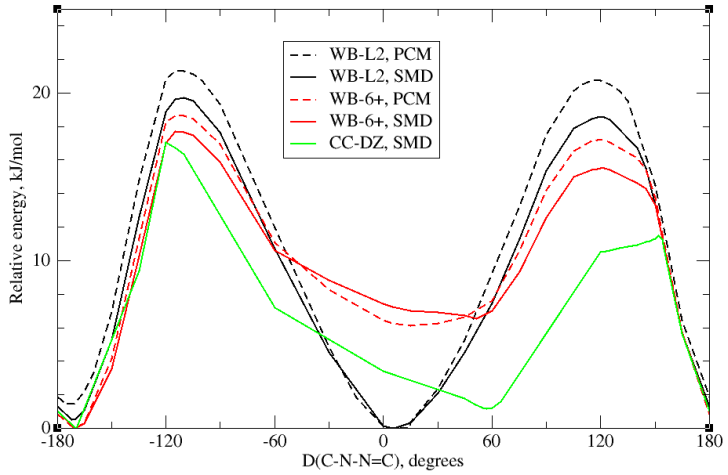

Figure S3. Potential energy curves of **M2**, calculated at different levels of theory. Energy relative to the lowest point on the curve.

1.3 Model 4 (**M4**)

Table S3. Properties of the potential energy curve of **M4**, calculated at different levels of theory. Energies are in kJ/mol; angles are in degrees. There are two barriers of interest (cf. Figure S3, below): "barrier$_1$" is at 0˚, "barrier$_2$" is at ~125-140˚.

Property:	WB-L2		WB-6+		CC-DZ	
	PCM	SMD	PCM	SMD	PCM	SMD
E_{syn}-E_{anti}	-1.93	0.4	2.6	2.9	-2.0	-1.6
$E_{barrier1}$-E_{syn}	–	–	2.6	4.6	1.9	3.8
$E_{barrier2}$-E_{syn}	14.0	11.7	6.6	6.1	9.4	8.6
syn- angle	0˚	0˚	65˚	67˚	62˚	66˚
barrier$_2$ angle	128˚	128˚	135˚	136˚	142˚	142˚

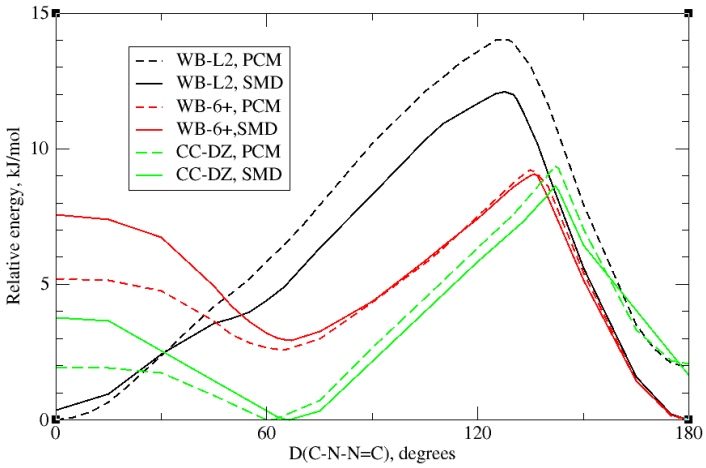

Figure S4. Potential energy curves of **M4**, calculated at different levels of theory.

1.4 Comments

For energy differences between *syn* and *anti*, neither WB-L2 nor WB-6+ consistently agree with CC-DZ; WB-6+ gives good results for **M1** but the *syn* form is about 2 mH too high (or *anti*, 2 mH too low) for **M2** and **M3**. For the energy barriers at ~105-135˚, WB-L2 consistently overestimates the height of the barrier, while WB-6+ does better.
The peak/shoulder at 0˚ for **M2** and **M4** is present at the coupled-cluster level; WB-L2 consistently fails to produce it, producing a curve that looks qualitatively different. WB-6+ with PCM underestimates this effect (too small a peak for **M4**, *syn*-angle too close to 0˚ for **M2**), but a slight shoulder is visible; WB-6+ with SMD gives a *syn*-angle close to CC-DZ for **M2** and **M4**, and for the latter also gives a similar height of the 0˚ energy maximum.

2. EXCITED STATES

2.1 Model 1 (**M1**)

Figure S5 below shows the unadjusted energy curves for M1's ground state and first four excited states, calculated at WB-6+/SMD level. For reasons discussed above, the excited state energies have a discontinuity around 107˚. The curves discussed in this section are vertical excitation energies; attempts to optimize the first two excited states (at WB-6+/SMD level) lead to extremely small energy gaps, and usually swapping of states, indicating conical intersections.

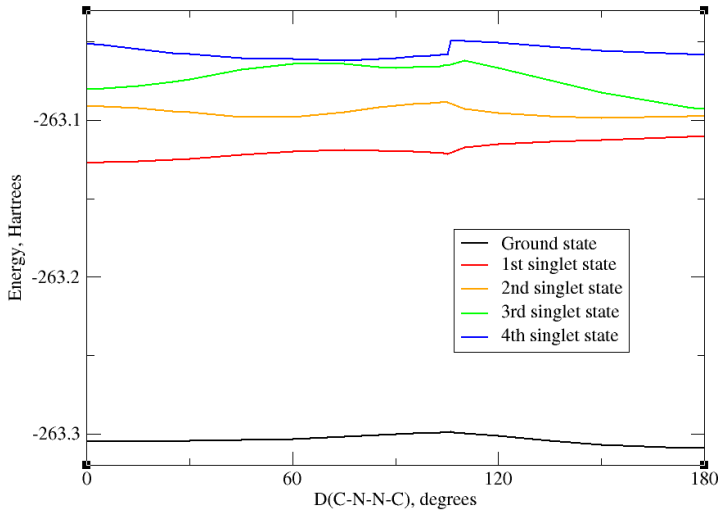

Figure S5. Unadjusted energy curves for **M1**: ground and excited states (vertical excitation energy curves), calculated using TD-DFT at the WB-6+, SMD level.

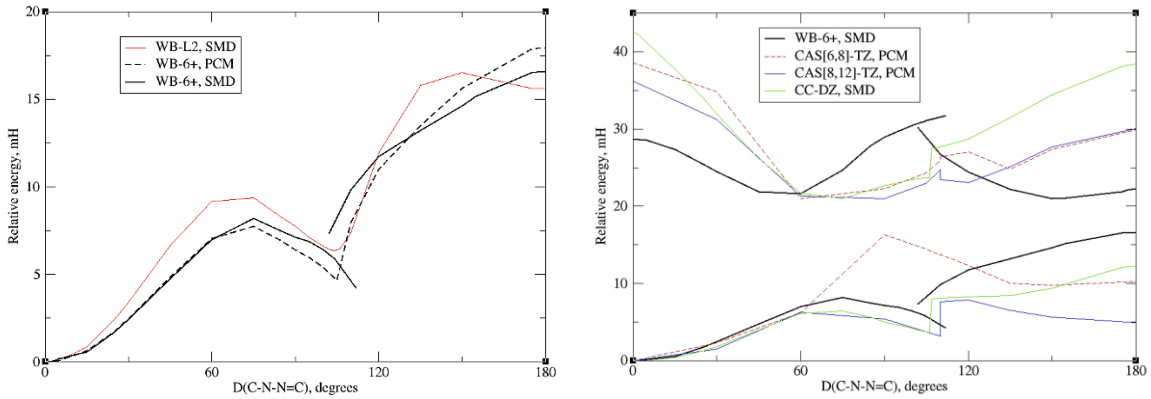

Figure S6. Vertical excitation energy curve for the first singlet excited state of **M1**, calculated at different levels of theory. Energy relative to syn-form (0˚). (Left) ES1, comparison of TD-DFT methods. (Right) ES1 and ES2, comparison of TD-DFT (WB-6+) with CAS-SCF and EOM-CCSD (CC-DZ); ES2 shifted by an arbitrary amount for clarity.

Figure S6 compares vertical excitation energy curves for different methods. For ES1, WB-6+ and EOM-CCSD predict a downhill slope away from the *anti*-conformer (180˚), whereas CASSCF predicts an uphill slope; for ES2, the curve slopes downhill from the *anti*-conformer according to all methods, but TD-DFT finds this extends only to about 150˚, whereas CASSCF finds it to be downhill to 120-135˚ (and EOM-CCSD finds it to extend still further).
The shapes of the vertical excitation energy curves are similar for TD-DFT, CASSCF and EOM-CCSD. However, examination of the first three excitations (for the anti-conformer) reveals that the character of the states is slightly different. For TD-DFT and CASSCF, the three excitations (in order) are HOMO-1 to LUMO; HOMO to LUMO; and HOMO-2 to LUMO. (For CASSCF, this was checked against CI-only calculations.) However, for EOM-CCSD, the second and third excited state are swapped around. Curiously, this does not seem to make much difference to the excitation energy curves for ES2 or ES3 (not shown).
In line with this, TD-DFT finds significant oscillator strength only for the 2nd excitation, whereas EOM-CCSD finds it only for the 3rd excitation. CAS[8,12], meanwhile, finds no significant oscillator strengths for the first three excitations.

Table S4. Excitation energies and oscillator strengths for **M1** at various levels of theory (anti-form). Calculated at TD-DFT (for WB-L2, WB-6+) or EOM-CCSD (for CC-DZ) level. CAS[8,12] results used state-averaging over the first 5 states; oscillator strengths given are dipole transition strengths, with velocity transition strengths given in brackets where different.

Excited state	Excitation energies					Oscillator strength				
	WB-L2, SMD	WB-6+, PCM	WB-6+, SMD	CC-DZ, SMD	CAS [8,12]	WB-L2, SMD	WB-6+, PCM	WB-6+, SMD	CC-DZ, SMD	CAS [8,12]
1	5.16	5.45	5.40	5.66	5.57	0.002	0.002	0.002	0.002	0.00
2	5.62	5.83	5.76	6.31	6.37	0.487	0.484	0.480	0.003	0.01(0.03)
3	5.72	5.90	5.89	6.47	8.02	0.000	0.000	0.000	0.475	0.01

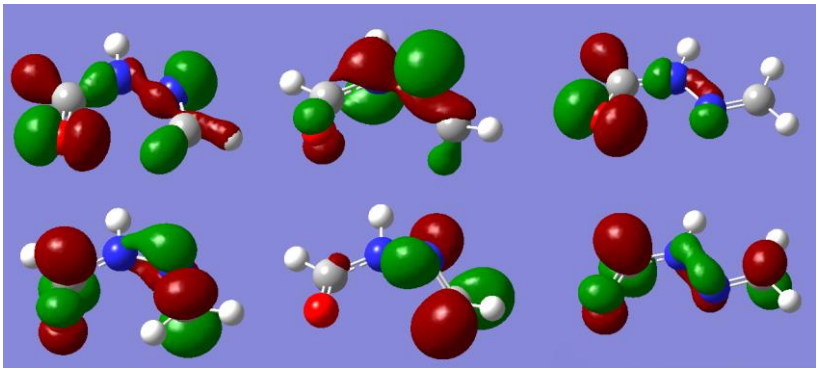

Figure S7. Natural Transition Orbitals (NTOs) for **M1**, first singlet excited state. Top row: Hole orbital. Bottom row: Excited orbital. Left: 0°. Middle: 90°. Right: 180°. Isosurface value: $10^{-1.19}$.

2.2 Model 2 (**M2**)

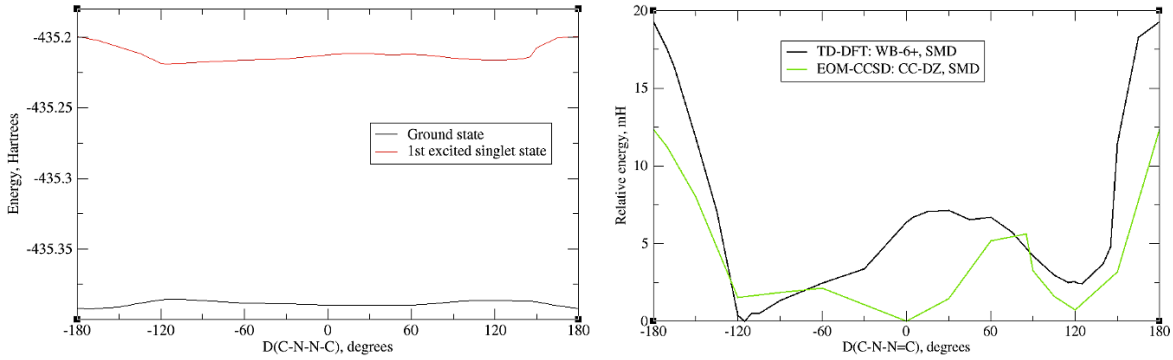

Figure 8 : (Left) unadjusted vertical excitation energy curves for **M2**: ground-state (GS), excited state 1 (ES1), calculated with TD-DFT: WB-6+; (Right) vertical excitation energy curves for **M2**, ES1, comparison of TD-DFT and EOM-CCSD.

Table S5. Excitation energies and oscillator strengths for **M2** (-170˚).

Excited state	WB-6+, SMD	
	Excitation energies	Oscillator strength
1	5.20	0.035
2	5.51	0.248
3	5.80	0.186

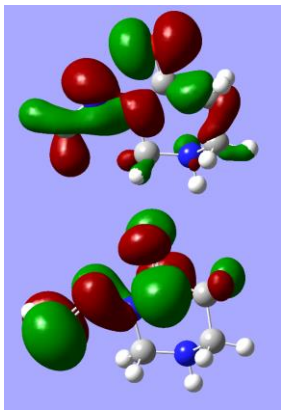

Figure S9. Natural Transition Orbitals for **M2**, anti-conformer (180˚). Isosurface value: 0.03.

2.3 Model 3 (**M1**), **S1**

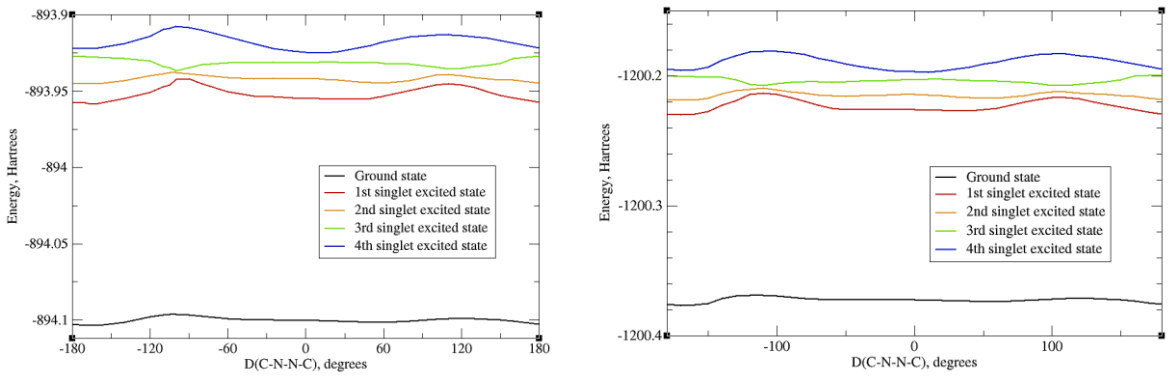

Figure S10. Unadjusted energy curves for **M3** (top), **S1** (bottom) for ground and excited states, calculated using TD-DFT at the WB-6+, SMD level.

Table S6. Excitation energies and transition probabilities for M3 and S1 (-170°), calculated using TD-DFT at the WB-6+, SMD level.

Excitation:	Excitation energy		Oscillator strength	
	M3	**S1**	**M3**	**S1**
1	3.96	3.99	0.533	0.478
2	4.31	4.29	0.223	0.236
3	4.79	4.79	0.279	0.295
4	4.93	4.92	0.025	0.016